Cell Metabolism
Short Article

Rapid Activation of Akt2 Is Sufficient to Stimulate GLUT4 Translocation in 3T3-L1 Adipocytes

Yvonne Ng,[1] Georg Ramm,[1] Jamie A. Lopez,[1] and David E. James[1,*]
[1]Diabetes and Obesity Research Program, Garvan Institute of Medical Research, Sydney, NSW 2010, Australia
*Correspondence: d.james@garvan.org.au
DOI 10.1016/j.cmet.2008.02.008

SUMMARY

The serine/threonine kinase Akt2 has been implicated in insulin-regulated glucose uptake into muscle and fat cells by promoting the translocation of glucose transporter 4 (GLUT4) to the cell surface. However, it remains unclear whether activation of Akt2 is sufficient since a role for alternate signaling pathways has been proposed. Here we have engineered 3T3-L1 adipocytes to express a rapidly inducible Akt2 system based on drug-inducible heterodimerization. Addition of the dimerizer rapalog resulted in activation of Akt2 within 5 min, concomitant with phosphorylation of the Akt substrates AS160 and GSK3. Comparison with insulin stimulation revealed that the level of Akt2 activity observed with rapalog was within the physiological range, reducing the likelihood of off-target effects. Transient activation of Akt2 also increased glucose transport and GLUT4 translocation to the plasma membrane. These results show that activation of Akt2 is sufficient to stimulate GLUT4 translocation in 3T3-L1 adipocytes to an extent similar to insulin.

INTRODUCTION

A major physiologic action of insulin is to promote glucose uptake into muscle and adipose tissue by triggering the translocation of the facilitative glucose transporter 4 (GLUT4) from intracellular compartments to the cell surface (Bryant et al., 2002). Defects in this process contribute to the development of insulin resistance in obesity and type 2 diabetes mellitus.

Insulin stimulation of the phosphatidylinositol 3-kinase (PI3K)/Akt pathway is necessary for insulin-stimulated glucose transport in both muscle and fat cells. Studies utilizing pharmacologic inhibitors such as wortmannin (Clarke et al., 1994) and LY294002 (Cheatham et al., 1994), Akt interfering antibodies and Akt substrate peptides (Hill et al., 1999), overexpression of dominant-negative Akt mutants and ablation of Akt via siRNA (Katome et al., 2003), and *Akt*$^{-/-}$ mice (Cho et al., 2001) and cell lines derived from these animals (Bae et al., 2003) have all shown that activation of Akt is necessary for insulin action. However, these studies do not exclude the possibility that other signaling pathways are also required. Indeed, several alternate pathways including c-Cbl/TC10 (Chiang et al., 2001), atypical protein kinase C (PKC) ζ/λ (Kotani et al., 1998), and Rac (Khayat et al., 2000) have been proposed to play an important role in GLUT4 translocation. These pathways are either activated upstream of Akt as a separate insulin-responsive pathway (c-Cbl/TC10) or diverge at the level of PI3K (PKCζ/λ and Rac). To address the role of the Akt pathway vis-à-vis alternate pathways, it is essential to show that activation of Akt alone is sufficient to mimic the effects of insulin. Previous studies have shown that overexpression of constitutively active Akt in 3T3-L1 adipocytes (Kohn et al., 1996), rat adipocytes (Tanti et al., 1997), and L6 muscle cells (Hajduch et al., 1998) can trigger GLUT4 translocation. However, these studies have been criticized because the cells used were exposed to high levels of activated Akt mutants for long periods of time prior to analysis, raising the possibility of indirect or non-physiological effects.

The use of a rapid inducible system that would result in activation of Akt independently of other pathways would provide a more rigorous approach to this problem. Roth and colleagues attempted to achieve this goal by expressing a tamoxifen-inducible Akt construct in 3T3-L1 adipocytes (Kohn et al., 1998). However, even here, activation of both Akt and GLUT4 translocation was only observed many hours after tamoxifen stimulation. These slow responses do not reflect insulin action in vivo, which occurs within minutes. Moreover, these studies employed the Akt1 isoform, and it is now clear that Akt2 is the major isoform involved in insulin action in muscle and fat cells (Cho et al., 2001; Hill et al., 1999).

To circumvent these problems, we have utilized a previously described drug-inducible heterodimerization strategy to acutely activate Akt2 in 3T3-L1 adipocytes. This strategy is based on the use of rapamycin to heterodimerize the rapamycin-binding domain of the FK506-binding protein 12 (FKBP12) and a 93 amino acid domain from FRAP/mTOR called FRB (*F*RAP *r*apamycin-*b*inding domain). A nonimmunosuppressive analog of rapamycin, known as rapalog (AP21967), has been developed to bind with high affinity to modified FRB containing a single amino acid change (Thr2098Leu) but not to endogenous mTOR. Therefore, addition of rapalog to cells expressing a myristoylated FKBP12 fragment and an FRB-Akt chimera induces rapid translocation of FRB-Akt to the plasma membrane, mimicking the effect of PI3K-induced translocation. This system has been used to study regulation of Akt activation (Scheid et al., 2002) and apoptosis (Li et al., 2002). This approach allows for a more physiological analysis, as it provides rapid activation of Akt2, avoiding the potential indirect consequences of long-term activation. It also bypasses potential upstream signaling pathways normally induced by insulin, allowing direct study of Akt2-regulated

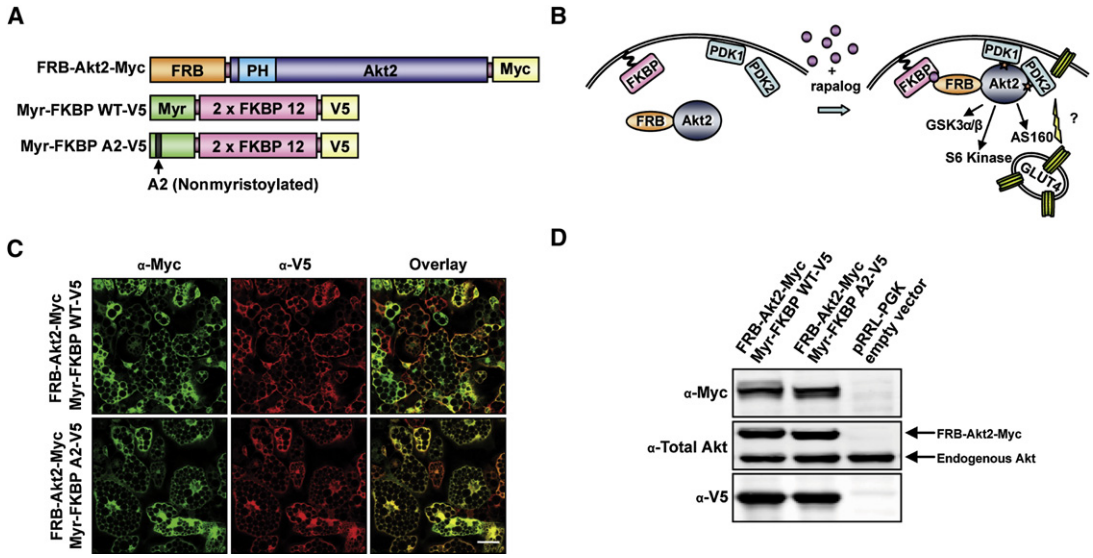

Figure 1. Development of a Rapalog-Inducible System for Regulated Akt2 Activation

(A) Schematic representation of chimeric constructs used in this study.

(B) Model of cell-permeable rapalog (AP21967)-mediated activation of FRB-Akt2 by crosslinking the FRB and FKBP domains, bringing the FRB-Akt2 fusion protein to the plasma membrane for its phosphorylation.

(C) Expression and localization of FRB-Akt2-Myc and Myr-FKBP WT-V5 or Myr-FKBP A2-V5 fusion proteins in 3T3-L1 adipocytes. Cells were labeled for immunofluorescence with anti-Myc or V5 antibodies followed by Cy2- and Cy3-conjugated secondary antibodies, respectively. Scale bar = 40 μM.

(D) SDS lysates of 3T3-L1 adipocytes expressing the control empty vector or FRB-Akt2-Myc and Myr-FKBP WT-V5 or Myr-FKBP A2-V5 lentivirus.

cellular processes in the absence of insulin. We took advantage of the lentivirus-mediated gene transfer technique to efficiently express transgenes in 3T3-L1 adipocytes. Akt2 was rapidly activated following addition of the dimerizer rapalog, and this activation was accompanied by robust phosphorylation of a range of Akt substrates as well as increased GLUT4 translocation and glucose transport.

RESULTS AND DISCUSSION

A System to Study Rapid Activation of Akt2 in 3T3-L1 Adipocytes

To acutely regulate the activity of Akt in 3T3-L1 adipocytes, we employed a drug-inducible heterodimerization system developed by ARIAD Pharmaceuticals. Full-length Akt2 was fused in-frame with the rapamycin-binding domain FRB (a mutated fragment from human FRAP/mTOR) to generate FRB-Akt2 (see Figure 1A). To effect membrane recruitment, a construct containing two copies of *FKBP12* with a *Src* myristoylation signal sequence at its amino terminus (FKBP WT) was generated (Figure 1A). In the presence of rapalog, a synthetic lipid-permeable nonbioactive drug, the two fusion proteins heterodimerize, recruiting FRB-Akt2 to the plasma membrane (Figure 1B). A control construct in which the myristoylated glycine at the second amino acid position was converted to alanine to eliminate the membrane-targeting function of the *Src* myristoylation signal sequence (FKBP A2) was also created (Figure 1A).

We explored a number of expression systems to fulfill the following criteria: FRB-Akt2 expression and Akt activation levels preferably within the range observed for endogenous Akt, to avoid off-target effects; maintenance of insulin responsiveness; and maximum efficiency of expression of both fusion proteins in 3T3-L1 adipocytes, thus facilitating metabolic studies in intact cells. We found that the lentiviral system was the only expression system that fulfilled these criteria. Infection of 3T3-L1 adipocytes with lentivirus expressing both FRB-Akt2 and FKBP WT or the FKBP A2 mutant resulted in >90% transduction (Figure 1C). Moreover, expression of these fusion proteins in 3T3-L1 adipocytes did not have any detectable toxic effects, nor did it modify the insulin responsiveness of the cells (data not shown), although we did observe a significant increase in cell size following lentiviral infection. However, this effect was Akt independent. The expression of fusion proteins was readily detected 3 days after transduction and remained stable for many weeks. The expression level of FRB-Akt2 was comparable to that of endogenous Akt. FKBP WT and the FKBP A2 mutant were also expressed at similar levels in 3T3-L1 adipocytes (Figure 1D).

Rapid Insulin-Independent Activation of FRB-Akt2 and Akt Substrates

We first examined the dose dependence of FRB-Akt2 activation by rapalog in 3T3-L1 adipocytes. Phosphorylation of FRB-Akt2 at Thr308 and Ser473 was observed using 20 nM rapalog, and the level of phosphorylation at both sites plateaued at 200–500 nM (Figure 2A). Importantly, we did not observe any significant phosphorylation of endogenous Akt in response to rapalog, nor did we observe phosphorylation of FRB-Akt2 in cells expressing the FKBP A2 mutant (Figure 2A). A similar dose-response curve for the phosphorylation of several downstream substrates of Akt was also observed in response to rapalog (Figure 2B). These data indicate that inducible recruitment of FRB-Akt2 to the plasma membrane in 3T3-L1 adipocytes is sufficient to activate Akt2 kinase activity, recapitulating the physiological actions of this kinase on a range of downstream substrates.

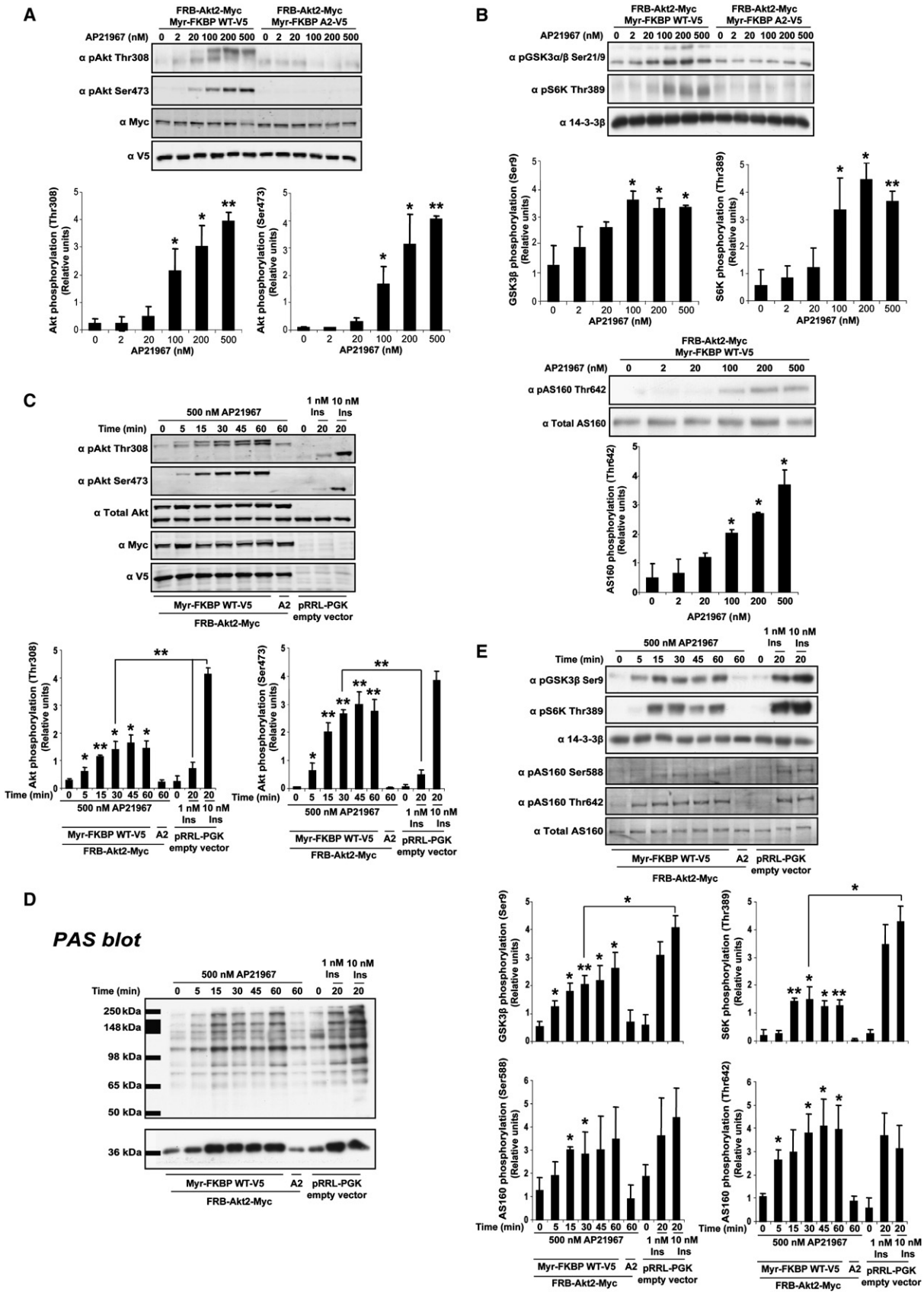
A
FRB-Akt2-Myc Myr-FKBP WT-V5
FRB-Akt2-Myc Myr-FKBP A2-V5
AP21967 (nM) 0 2 20 100 200 500 0 2 20 100 200 500
α pAkt Thr308
α pAkt Ser473
α Myc
α V5
Akt phosphorylation (Thr308) (Relative units)
Akt phosphorylation (Ser473) (Relative units)
AP21967 (nM)
B
FRB-Akt2-Myc Myr-FKBP WT-V5
FRB-Akt2-Myc Myr-FKBP A2-V5
AP21967 (nM) 0 2 20 100 200 500 0 2 20 100 200 500
α pGSK3α/β Ser21/9
α pS6K Thr389
α 14-3-3β
GSK3β phosphorylation (Ser9) (Relative units)
S6K phosphorylation (Thr389) (Relative units)
AP21967 (nM)
FRB-Akt2-Myc Myr-FKBP WT-V5
AP21967 (nM) 0 2 20 100 200 500
α pAS160 Thr642
α Total AS160
AS160 phosphorylation (Thr642) (Relative units)
AP21967 (nM)
C
500 nM AP21967
1 nM Ins 10 nM Ins
Time (min) 0 5 15 30 45 60 60 0 20 20
α pAkt Thr308
α pAkt Ser473
α Total Akt
α Myc
α V5
Myr-FKBP WT-V5 A2 pRRL-PGK empty vector
FRB-Akt2-Myc
Akt phosphorylation (Thr308) (Relative units)
Akt phosphorylation (Ser473) (Relative units)
Time (min) 0 5 15 30 45 60 60 0 20 20
500 nM AP21967
1 nM Ins 10 nM Ins
Myr-FKBP WT-V5 A2 pRRL-PGK empty vector
FRB-Akt2-Myc
D
PAS blot
500 nM AP21967
1 nM Ins 10 nM Ins
Time (min) 0 5 15 30 45 60 60 0 20 20
250 kDa
148 kDa
98 kDa
65 kDa
50 kDa
36 kDa
Myr-FKBP WT-V5 A2 pRRL-PGK empty vector
FRB-Akt2-Myc
E
500 nM AP21967
1 nM Ins 10 nM Ins
Time (min) 0 5 15 30 45 60 60 0 20 20
α pGSK3β Ser9
α pS6K Thr389
α 14-3-3β
α pAS160 Ser588
α pAS160 Thr642
α Total AS160
Myr-FKBP WT-V5 A2 pRRL-PGK empty vector
FRB-Akt2-Myc
GSK3β phosphorylation (Ser9) (Relative units)
S6K phosphorylation (Thr389) (Relative units)
AS160 phosphorylation (Ser588) (Relative units)
AS160 phosphorylation (Thr642) (Relative units)
Time (min) 0 5 15 30 45 60 60 0 20 20
500 nM AP21967
1 nM Ins 10 nM Ins
Myr-FKBP WT-V5 A2 pRRL-PGK empty vector
FRB-Akt2-Myc

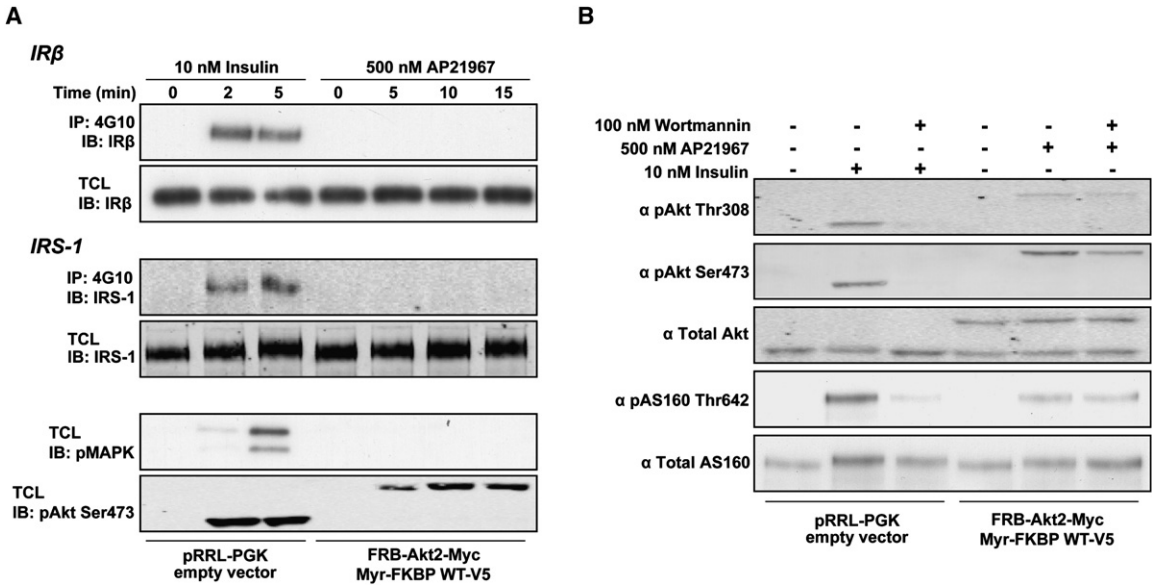

Figure 3. Rapalog-Induced Activation of FRB-Akt2 Is Independent of Insulin Receptor Signaling in 3T3-L1 Adipocytes

(A) IRβ, IRS-1, and MAPK are not activated by Akt2. 3T3-L1 adipocytes transduced with the respective lentivirus were serum starved for 2 hr and stimulated with 10 nM insulin or 500 nM rapalog for the indicated times. Cell lysates were prepared and tyrosine-phosphorylated proteins were immunoprecipitated with anti-phosphotyrosine antibody (4G10). The immune complexes were then immunoblotted with anti-IRβ or anti-IRS-1 antibodies. Total cell lysates (TCL) were also immunoblotted for total IRβ, total IRS-1, pMAPK, and pAkt Ser473. Immunoblots shown are from a representative experiment (n = 3).

(B) Activation of FRB-Akt2 is independent of PI3K. 3T3-L1 adipocytes transduced with the respective lentivirus were serum starved for 2 hr and stimulated with 100 nM wortmannin or vehicle (DMSO, final concentration 0.1%) for 30 min before stimulation with or without 10 nM insulin or 500 nM rapalog for 30 min. Total cell lysates were immunoblotted with antibodies directed against pAkt Thr308, pAkt Ser473, total Akt, pAS160 Thr642, or total AS160. Immunoblots shown are from a representative experiment (n = 3).

We next examined the kinetics of FRB-Akt2 activation in response to rapalog. Significant phosphorylation of FRB-Akt2 at Thr308 and Ser473 was observed 5 min after addition of rapalog, reaching a plateau by 15 min (Figure 2C). For comparison, we also examined insulin-stimulated phosphorylation of endogenous Akt in parallel. Importantly, the level of rapalog-induced phosphorylation of FRB-Akt2 at Ser473 was similar to insulin-stimulated phosphorylation of endogenous Akt at 10 nM insulin (Figure 2C). Notably, rapalog-induced phosphorylation at Thr308 was significantly less than insulin-stimulated (10 nM) phosphorylation of endogenous Akt at the same site. However, this likely reflects the differential affinity of these antibodies for Akt1 versus Akt2, both isoforms being expressed in 3T3-L1 adipocytes (Hill et al., 1999). Using phospho-Akt substrate (PAS) antibody, addition of rapalog to 3T3-L1 adipocytes triggered the phosphorylation of a range of downstream substrates similar to that observed with insulin (Figure 2D). We also observed rapid phosphorylation of GSK3, S6 kinase (S6K), and AS160, a recently identified substrate of Akt (Sano et al., 2003), at two separate Akt phosphorylation sites following rapalog addition, although the phosphorylation of Thr389 in S6K and Ser588 in AS160 was slower than that of either Ser9 in GSK3β or Thr642 in AS160 (Figure 2E). Moreover, whereas the amplitude of AS160 phosphorylation was similar to that observed with 10 nM insulin, this was not the case for either S6K or GSK3 (Figure 2E). This may reflect differential subcellular targeting of these substrates with respect to the FRB-Akt2 construct or a differential role for Akt1 versus Akt2 in signaling to its selective substrates. We also performed similar comparative studies using a more physiological dose of insulin (1 nM; James et al., 1985) in which we also obtained similar activation of Akt and AS160 phosphorylation (see Figure S1 available online). One other discrepancy highlighted by these studies was the spareness in signaling. At 1 nM insulin, we observed that endogenous Akt phosphorylation was barely detectable whereas AS160 phosphorylation at Thr642 was similar to that observed at 10 nM insulin (Figures 2C and 2E).

Rapalog-Induced Activation of FRB-Akt2 Is Independent of Insulin Receptor Signaling

Rapalog addition to 3T3-L1 adipocytes specifically activated the Akt pathway independently of the insulin receptor (Figure 3A). We were unable to detect significant tyrosine phosphorylation

Figure 2. Rapalog-Induced Activation of FRB-Akt2 and Akt2 Downstream Signaling

(A and B) Dose-dependent activation of FRB-Akt2 and Akt2 downstream signaling. 3T3-L1 adipocytes transduced with the indicated lentivirus were serum starved for 2 hr and treated with different concentrations of rapalog (AP21967) for 15 min. Total cell lysates were immunoblotted with antibodies raised against phospho-Akt (pAkt) Thr308, pAkt Ser473, and the Myc and V5 epitopes (A) or pGSK3 α/β Ser21/9, pS6K Thr389, 14-3-3β, pAS160 Thr642, and total AS160 (B).

(C–E) Time course of FRB-Akt2 activation and Akt2 downstream signaling. 3T3-L1 adipocytes were stimulated with 500 nM rapalog or 1 nM or 10 nM insulin for the indicated times. Total cell lysates were immunoblotted with antibodies directed against pAkt Thr308, pAkt Ser473, total Akt, and the Myc and V5 epitopes (C); phospho-Akt substrate (PAS) (D); or pGSK3β Ser9, pS6K Thr389, 14-3-3β, pAS160 Ser588, pAS160 Thr642, and total AS160 (E).

Data are presented as means ± SD. *$p < 0.05$, **$p < 0.01$ versus no treatment, or as indicated, by Student's t test (n = 3).

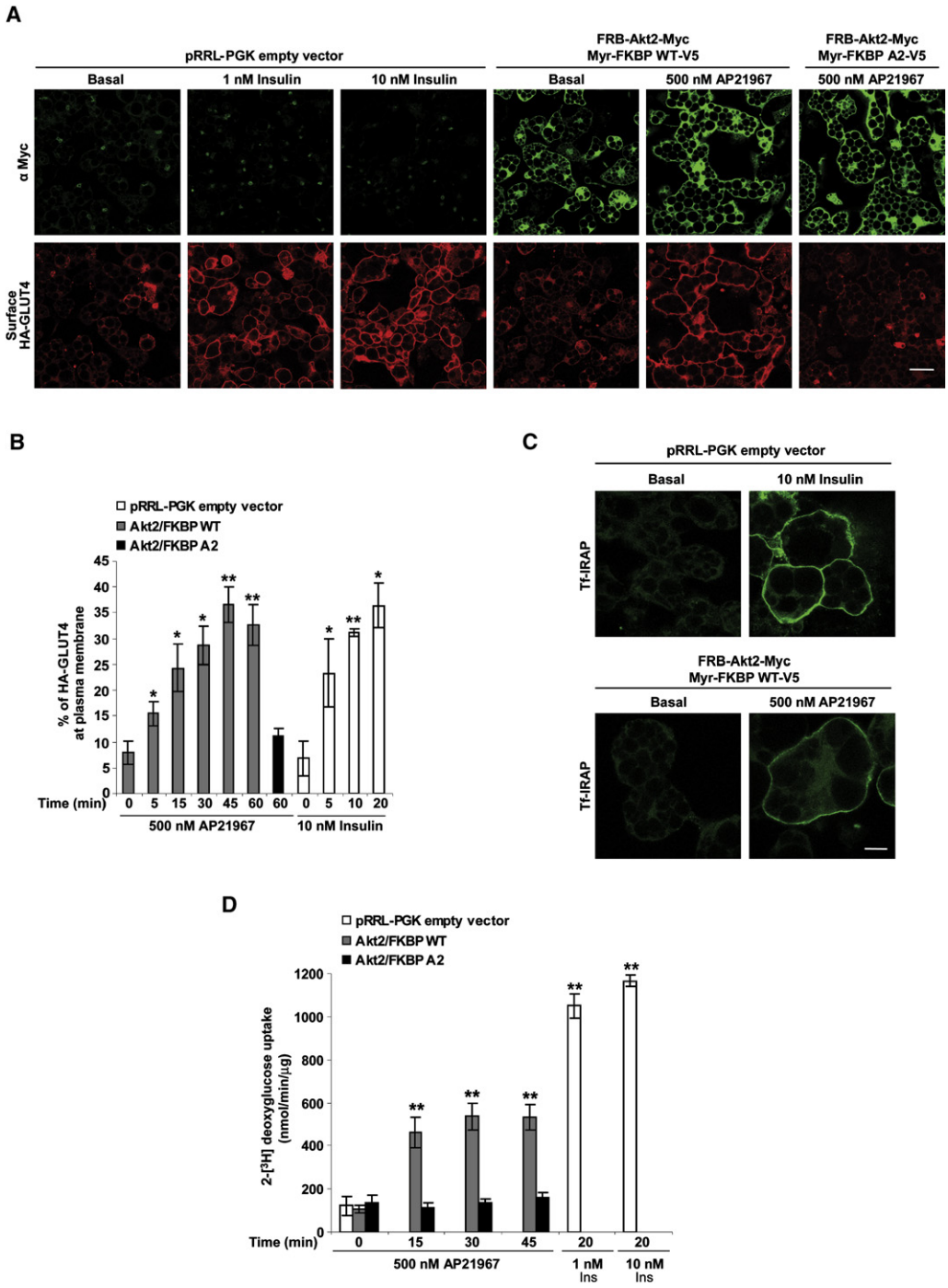

Figure 4. Rapalog-Induced GLUT4 and IRAP Translocation and Glucose Uptake in 3T3-L1 Adipocytes

(A) 3T3-L1 adipocytes expressing HA-GLUT4 were transduced with the respective lentivirus and serum starved for 2 hr before stimulation with 1 nM or 10 nM insulin for 20 min or 500 nM rapalog for 30 min. The amount of HA-GLUT4 at the plasma membrane was determined by labeling with anti-HA antibody in combination with Cy3-conjugated secondary antibody in nonpermeabilized cells. Cells were then permeabilized, and cells transduced with FRB-Akt2-Myc lentivirus were detected with anti-Myc followed by Cy2-conjugated secondary antibody. Images are from a representative experiment (n = 3). Scale bar = 40 μM.

(B) HA-GLUT4-expressing 3T3-L1 adipocytes grown in 96-well plates were transduced with lentivirus and stimulated for the indicated periods with 10 nM insulin or 500 nM rapalog. The amount of HA-GLUT4 at the plasma membrane was determined by anti-HA fluorescence immunolabeling of nonpermeabilized cells and expressed as a percentage of total cellular HA-GLUT4 as determined by labeling of permeabilized cells. Data are presented as means ± SD. *$p < 0.05$, **$p < 0.01$ versus no treatment by Student's t test (n = 3).

(C) Tf-IRAP-expressing 3T3-L1 adipocytes transduced with lentivirus were stimulated with 10 nM insulin or 500 nM rapalog for 30 min. Surface Tf-IRAP was analyzed by labeling with Alexa 488-Tf. Scale bar = 20 μM.

of the insulin receptor (IRβ) or insulin receptor substrate-1 (IRS-1) in response to rapalog in 3T3-L1 adipocytes expressing FRB-Akt2 and FKBP WT. In addition, we were unable to detect any significant activation of the mitogen-activated protein kinase (MAPK) pathway in response to rapalog, which is activated in response to insulin in an Akt-independent manner. Furthermore, in the presence of the PI3K inhibitor wortmannin, rapalog-stimulated phosphorylation of Akt and AS160 was not inhibited (Figure 3B).

Activation of FRB-Akt2 Stimulates GLUT4 and IRAP Translocation and Glucose Uptake in 3T3-L1 Adipocytes

The above studies suggest that the dimerization system can be adapted to 3T3-L1 adipocytes to study the specific function of Akt2 in these cells under physiological conditions in terms of both the kinetics and amplitude of Akt activation. Hence, we next asked whether induced activation of Akt2 was sufficient to stimulate HA-GLUT4 translocation as described previously (Govers et al., 2004) and glucose transport in 3T3-L1 adipocytes. In unstimulated 3T3-L1 adipocytes transduced with an empty lentivirus, HA-GLUT4 was predominantly retained within cells. A significant redistribution of this reporter to the cell surface was observed in response to either 1 nM or 10 nM insulin (Figure 4A). Strikingly, a similar level of HA-GLUT4 translocation to the cell surface was observed in response to rapalog in 3T3-L1 adipocytes expressing FRB-Akt2 and FKBP WT (Figures 4A and 4B). Conversely, no significant HA-GLUT4 translocation was observed in response to rapalog in cells expressing FRB-Akt2 and the FKBP A2 mutant (Figures 4A and 4B). To confirm that these effects were not specific to GLUT4, we also showed that rapalog stimulated the translocation of the insulin-regulated aminopeptidase (IRAP) reporter transferrin receptor-IRAP (Tf-IRAP) to the plasma membrane in a manner similar to that observed with insulin (Figure 4C; Gonzalez and McGraw, 2006). The time course of rapalog-stimulated GLUT4 translocation was slightly delayed compared to insulin (Figure 4B), but this paralleled Akt activation (Figure 2C). In contrast to the observations with insulin, rapalog-stimulated GLUT4 translocation was unaffected by the PI3K inhibitor wortmannin (Figure S2).

We next examined the effect of rapalog on glucose transport in 3T3-L1 adipocytes. Incubation of 3T3-L1 adipocytes that were transduced with control lentivirus with 1 nM or 10 nM insulin resulted in an increase in 2-deoxyglucose uptake by ~8.5- and ~9.5-fold, respectively (Figure 4D). Intriguingly, the dose response of insulin-stimulated 2-deoxyglucose uptake paralleled the dose-response activation of AS160 phosphorylation, but not that of Akt itself (Figures 2C and 2E). Hence, these data confirm that minimal activation of Akt is sufficient to elicit a maximum effect on glucose transport and AS160 phosphorylation. With regard to the latter, it is noteworthy that we did not measure the amount of nonphosphorylated AS160 under these conditions, and so it remains unclear whether the total AS160 pool is phosphorylated in response to maximal stimulation. Hence, it remains possible that the discrete subcellular distribution of activated Akt to a pool of AS160 that has to be inactivated in order to allow GLUT4 translocation may play an important role. This may be relevant in light of recent studies that found an incomplete inhibitory effect of Akt inhibition on GLUT4 translocation (Gonzalez and McGraw, 2006; Jiang et al., 2003). Infection of 3T3-L1 adipocytes with FRB-Akt2 and FKBP lentivirus had no significant effect on basal 2-deoxyglucose uptake (Figure 4D). Rapalog stimulation of 3T3-L1 adipocytes expressing FRB-Akt2 and the FKBP A2 mutant did not result in any significant increase in glucose uptake at any time tested (Figure 4D), consistent with the lack of activation of Akt2 and HA-GLUT4 translocation (Figure 2C; Figure 4B). Exposure of cells expressing FRB-Akt2 and FKBP WT to 500 nM rapalog for 15 min resulted in an ~4.5-fold increase in glucose uptake, which was maintained after 30 min and 45 min of stimulation (Figure 4D). Interestingly, in contrast to AS160 phosphorylation (Figure 2E) and HA-GLUT4 translocation (Figure 4B), rapalog-stimulated 2-deoxyglucose uptake was less than that observed with insulin. It is unlikely that this is due to the inability of rapalog to stimulate GLUT1 translocation. In contrast to previous studies (Foran et al., 1999), we observed that insulin-stimulated GLUT1 translocation was inhibited by wortmannin and an Akt inhibitor (Figure S3) in agreement with studies in *Akt2* knockout mice (Bae et al., 2003). Perhaps a more likely scenario is that the Akt-dependent movement of GLUT4 to the plasma membrane may not be sufficient for full transport activation, implicating an additional step in this process (Hausdorff et al., 1999).

These data support the notion that rapid activation of Akt2 is sufficient to stimulate GLUT4 translocation in 3T3-L1 adipocytes. We also observed no additivity between rapalog and insulin on glucose transport (Figure S4), indicating that these agents likely trigger GLUT4 translocation via the same mechanism. The inducible system employed was designed to replicate the physiological effects of insulin in terms of kinetics and amplitude of the Akt response. This would place glucose transport in line with many other metabolic actions of insulin including glycogen synthesis, protein synthesis, and lipogenesis that also appear to rely principally upon Akt for their activation (Whiteman et al., 2002). Hence, this positions Akt at a major node in the regulation of metabolism by insulin.

Several other signaling pathways have been implicated in insulin-regulated glucose transport. One of these is the PI3K-independent c-Cbl/TC10/CIP4/2 pathway, which has been suggested to operate in parallel to the PI3K/Akt pathway (Chiang et al., 2001). However, other studies have not been able to show an inhibition of insulin-stimulated glucose transport using siRNA knockdown of various members of the pathway (Mitra et al., 2004) or in c-*Cbl*$^{-/-}$ mice (Molero et al., 2004). In addition, PI3K-dependent activation of Ral A and the exocyst complex have been implicated in targeting GLUT4 vesicles to the cell surface (Chen et al., 2007). More recently, an important role for the atypical PKCλ in insulin-stimulated glucose uptake has been suggested. Muscle-specific deletion of *PKC*λ results in a profound inhibition of insulin-stimulated glucose transport into muscle without any apparent defect in insulin-stimulated Akt activation (Farese et al., 2007). The relevance of these observations with respect to the present study remains to be defined. One possibility is that in addition to Akt activation, only a basal level

(D) 3T3-L1 adipocytes transduced with lentivirus were stimulated with 500 nM rapalog or 1 nM or 10 nM insulin for the indicated times, and 2-[^{3}H]deoxyglucose uptake was determined. Data are presented as means ± SD. **$p < 0.01$ versus no treatment by Student's t test ($n = 3$).

of activity of some of these factors is necessary for GLUT4 translocation. Notably, many of these studies have relied on the use of inhibitors that block insulin action, whereas the use of inducible systems for studying the effects of rapid activation of these signaling molecules on GLUT4 translocation has yet to be reported.

The observation that activation of Akt is sufficient to stimulate GLUT4 translocation suggests that identification of additional Akt substrates in adipocytes will be fruitful. However, recent functional studies in adipocytes suggest that the Akt substrate Rab GTPase-activating protein AS160 may not be the only regulated target of insulin (Bai et al., 2007; Gonzalez and McGraw, 2006). Based on the present study, we suggest that there may be alternate substrates of Akt that play an important role in this process, and so the present study lays the groundwork for future studies in this area.

EXPERIMENTAL PROCEDURES

Construction of Lentiviral Vectors

The ARGENT Regulated Transcription Retrovirus Kit (version 2.0) was obtained from ARIAD Pharmaceuticals. The cDNA encoding the full-length human *Akt2* was amplified by polymerase chain reaction (PCR) with a 3′ primer containing the *Myc* epitope tag and then cloned into pC_4-R_HE vector (ARIAD) in-frame with the rapamycin-binding domain *FRB* to produce FRB-Akt2-Myc. To generate the lentiviral expression vector, the resulting FRB-Akt2-Myc was subcloned into the lentiviral vector pRRL-PGK. The myristoylated rapamycin-binding domains were generated by PCR amplification of the rapamycin-binding domains (*FKBP12*) from pC_4M-F2E vector (ARIAD) using a 3′ primer containing the *V5* epitope tag and subcloned into a separate pRRL-PGK lentiviral vector (FKBP WT). A negative control construct (FKBP A2) was created by site-directed mutagenesis changing the glycine at the amino acid position 2 of the *Src* myristoylation sequence to alanine. The plasmids were verified by PCR sequencing. The pRRL-PGK lentiviral expression vector was generously provided by R. Hoeben (Leiden University Medical Center, The Netherlands), and the packaging vectors pMDLg/pRRE (gag/pol vector), pRSV-Rev (rev vector), and pMD2.G (VSV-G vector) were from D. Trono (Ecole Polytechnique Fédérale de Lausanne, Switzerland).

Cell Culture and Lentiviral Infection

3T3-L1 fibroblasts (ATCC) were cultured and differentiated into adipocytes as described previously (Larance et al., 2005). 3T3-L1 fibroblasts were infected with pBabepuro-HA-GLUT4 or pBabepuro-HA-GLUT1 retrovirus as described previously (Shewan et al., 2003). Recombinant lentiviruses were produced by cotransfecting HEK293 FT cells (Invitrogen) with lentiviral expression and packaging plasmids using the calcium phosphate transfection method as described previously (Carlotti et al., 2004; Li and Rossi, 2005). Infectious lentiviruses were harvested at 24 and 48 hr posttransfection and centrifuged at 1620 × g for 10 min. The supernatant collected was concentrated 10-fold using Amicon Ultracel concentration tubes (100 kDa pore size; Millipore). 3T3-L1 adipocytes at day 5 of differentiation were infected with 50 μl/well (for 96-well plate), 200 μl/well (for 24-well plate), or 960 μl/well (for 6-well plate) of concentrated empty vector or FRB-Akt2 lentivirus containing 4 μg/ml of polybrene. After 16–24 hr, the concentrated lentivirus was removed and replaced with fresh culture medium. For 3T3-L1 adipocytes requiring double infection, cells were infected again with either concentrated FKBP WT or FKBP A2 lentivirus. Experiments were performed at 5 days posttransduction.

Immunoprecipitation and Western Blot Analysis

After treatments, cells were washed twice with ice-cold PBS and solubilized in 2% SDS in PBS with phosphatase inhibitors (1 mM sodium pyrophosphate, 2 mM sodium vanadate, 10 mM sodium fluoride) and Complete protease inhibitor mixture (Roche). Insoluble material was removed by centrifugation at 18,000 × g for 10 min, and proteins were then separated by SDS-PAGE and transferred to polyvinylidene difluoride membranes (Millipore). Membranes were incubated in blocking buffer (BB) containing 5% BSA in 0.1% Tween 20 in Tris-buffered saline and immunoblotted with respective antibodies overnight at 4°C in BB. After incubation, membranes were washed and incubated with horseradish peroxidase-labeled secondary antibodies (Amersham) and then detected by SuperSignal West Pico chemiluminescent substrate (Pierce). In some cases, IR dye 700- or 800-conjugated secondary antibodies (Rockland Immunochemicals) were used. Membranes were then scanned in the 700 nM or 800 nM channel using an Odyssey IR imager. Quantification of protein levels was performed using Odyssey IR imaging system software.

For immunoprecipitation, cells after treatments were subsequently washed twice with ice-cold PBS before solubilization for 20 min at 4°C in RIPA buffer (50 mM Tris [pH 7.5], 150 mM NaCl, 1% Triton X-100, 0.5% sodium deoxycholate, 0.1% SDS, 1 mM EDTA, 10% glycerol) with phosphatase inhibitors and Complete protease inhibitor mixture. Lysates obtained after centrifugation at 18,000 × g for 20 min were incubated with 2 μg of anti-phosphotyrosine antibody or nonimmunized mouse IgG overnight at 4°C. The antibodies were then captured with protein G Sepharose beads (Pierce) for 2 hr, and immunoprecipitates were washed extensively with ice-cold RIPA buffer and boiled in SDS sample buffer.

2-Deoxyglucose Uptake

2-deoxyglucose uptake into 3T3-L1 adipocytes was performed as described previously (van Dam et al., 2005).

Immunofluorescence Microscopy

For detection of double infection, 3T3-L1 adipocytes were permeabilized and immunolabeled with polyclonal Myc antibody and monoclonal V5 antibody to detect FRB-Akt2-Myc and Myr-FKBP WT-V5 or Myr-FKBP A2-V5, respectively. Primary antibodies were detected with anti-rabbit Cy2- and anti-mouse Cy3-conjugated secondary antibodies. To determine HA-GLUT4 surface labeling, cells after treatments were washed in ice-cold PBS, fixed, and immunolabeled for surface HA-GLUT4 using monoclonal HA antibody. Cells were then permeabilized with saponin and immunolabeled with polyclonal anti-Myc antibody to identify cells infected with FRB-Akt2-Myc. Primary antibodies were detected with anti-mouse Cy3- and anti-rabbit Cy2-conjugated secondary antibodies. Optical sections were obtained through sequential scans for Cy2 (excitation 488 nm) and Cy3 (excitation 543 nm) using a Leica DM IRE2 TCS SP2 AOBS confocal laser scanning microscope with a 63× NA/1.32 CS oil HCX PL APO objective.

Quantitative GLUT4 Translocation Assay

HA-GLUT4 translocation to the plasma membrane was measured as described previously (Govers et al., 2004). Briefly, lentivirally infected 3T3-L1 adipocytes stably expressing HA-GLUT4 in 96-well plates were starved for 2 hr in serum- and bicarbonate-free DMEM containing 20 mM HEPES (pH 7.4) and 0.2% BSA. After stimulation, cells were fixed and immunolabeled with monoclonal anti-HA antibody followed by Alexa 488-labeled secondary antibody in the absence or presence of saponin to analyze the amount of HA-GLUT4 at the plasma membrane or the total HA-GLUT4 content, respectively.

Tf-IRAP Translocation Measured by Fluorescence Microscopy

Lentivirally infected 3T3-L1 adipocytes stably expressing a Tf-IRAP chimera (Lampson et al., 2000) were stimulated with either rapalog or insulin. Cells were washed with ice-cold DMEM, incubated with Alexa 488-Tf for 1 hr in DMEM with 20 mM HEPES (pH 7.4) and 0.2% BSA at 4°C, and then fixed in paraformaldehyde. Images were collected and processed as above.

Statistical Analysis

Data are expressed as means ± standard deviation (SD). p values were calculated by two tailed Student's t test using Microsoft Excel.

SUPPLEMENTAL DATA

Supplemental Data include four figures and can be found with this article online at http://www.cellmetabolism.org/cgi/content/full/7/4/348/DC1/.

ACKNOWLEDGMENTS

We thank R. Piper and J. Stöckli for invaluable discussions, C. Hohnen-Behrens for help with the GLUT4 translocation experiments, P. Shepherd (Symansis, Auckland, New Zealand) for the kind gifts of phospho-AS160 antibodies and the Akt inhibitor, T. McGraw for providing the Tf-IRAP cDNA, A. Cooper and A. Swarbrick for critical review of the manuscript, and ARIAD Pharmaceuticals (http://www.ariad.com/wt/page/regulation_kits) for generously providing AP21967 and the FRB and FKBP template DNA. This work was supported by grants from the National Health and Medical Research Council (NHMRC) of Australia. D.E.J. is an NHMRC Senior Principal Research Fellow.

Received: September 14, 2007
Revised: December 24, 2007
Accepted: February 14, 2008
Published: April 8, 2008

REFERENCES

Bae, S.S., Cho, H., Mu, J., and Birnbaum, M.J. (2003). Isoform-specific regulation of insulin-dependent glucose uptake by Akt/protein kinase B. J. Biol. Chem. *278*, 49530–49536.

Bai, L., Wang, Y., Fan, J., Chen, Y., Ji, W., Qu, A., Xu, P., James, D.E., and Xu, T. (2007). Dissecting multiple steps of GLUT4 trafficking and identifying the sites of insulin action. Cell Metab. *5*, 47–57.

Bryant, N.J., Govers, R., and James, D.E. (2002). Regulated transport of the glucose transporter GLUT4. Nat. Rev. Mol. Cell Biol. *3*, 267–277.

Carlotti, F., Bazuine, M., Kekarainen, T., Seppen, J., Pognonec, P., Maassen, J.A., and Hoeben, R.C. (2004). Lentiviral vectors efficiently transduce quiescent mature 3T3-L1 adipocytes. Mol. Ther. *9*, 209–217.

Cheatham, B., Vlahos, C.J., Cheatham, L., Wang, L., Blenis, J., and Kahn, C.R. (1994). Phosphatidylinositol 3-kinase activation is required for insulin stimulation of pp70 S6 kinase, DNA synthesis, and glucose transporter translocation. Mol. Cell. Biol. *14*, 4902–4911.

Chen, X.W., Leto, D., Chiang, S.H., Wang, Q., and Saltiel, A.R. (2007). Activation of RalA is required for insulin-stimulated Glut4 trafficking to the plasma membrane via the exocyst and the motor protein Myo1c. Dev. Cell *13*, 391–404.

Chiang, S.H., Baumann, C.A., Kanzaki, M., Thurmond, D.C., Watson, R.T., Neudauer, C.L., Macara, I.G., Pessin, J.E., and Saltiel, A.R. (2001). Insulin-stimulated GLUT4 translocation requires the CAP-dependent activation of TC10. Nature *410*, 944–948.

Cho, H., Mu, J., Kim, J.K., Thorvaldsen, J.L., Chu, Q., Crenshaw, E.B., 3rd, Kaestner, K.H., Bartolomei, M.S., Shulman, G.I., and Birnbaum, M.J. (2001). Insulin resistance and a diabetes mellitus-like syndrome in mice lacking the protein kinase Akt2 (PKB beta). Science *292*, 1728–1731.

Clarke, J.F., Young, P.W., Yonezawa, K., Kasuga, M., and Holman, G.D. (1994). Inhibition of the translocation of GLUT1 and GLUT4 in 3T3-L1 cells by the phosphatidylinositol 3-kinase inhibitor, wortmannin. Biochem. J. *300*, 631–635.

Farese, R.V., Sajan, M.P., Yang, H., Li, P., Mastorides, S., Gower, W.R., Nimal, S., Choi, C.S., Kim, S., Shulman, G.I., et al. (2007). Muscle-specific knockout of PKC-lambda impairs glucose transport and induces metabolic and diabetic syndromes. J. Clin. Invest. *117*, 2289–2301.

Foran, P.G., Fletcher, L.M., Oatey, P.B., Mohammed, N., Dolly, J.O., and Tavare, J.M. (1999). Protein kinase B stimulates the translocation of GLUT4 but not GLUT1 or transferrin receptors in 3T3-L1 adipocytes by a pathway involving SNAP-23, synaptobrevin-2, and/or cellubrevin. J. Biol. Chem. *274*, 28087–28095.

Gonzalez, E., and McGraw, T.E. (2006). Insulin signaling diverges into Akt-dependent and -independent signals to regulate the recruitment/docking and the fusion of GLUT4 vesicles to the plasma membrane. Mol. Biol. Cell *17*, 4484–4493.

Govers, R., Coster, A.C., and James, D.E. (2004). Insulin increases cell surface GLUT4 levels by dose dependently discharging GLUT4 into a cell surface recycling pathway. Mol. Cell. Biol. *24*, 6456–6466.

Hajduch, E., Alessi, D.R., Hemmings, B.A., and Hundal, H.S. (1998). Constitutive activation of protein kinase B alpha by membrane targeting promotes glucose and system A amino acid transport, protein synthesis, and inactivation of glycogen synthase kinase 3 in L6 muscle cells. Diabetes *47*, 1006–1013.

Hausdorff, S.F., Fingar, D.C., Morioka, K., Garza, L.A., Whiteman, E.L., Summers, S.A., and Birnbaum, M.J. (1999). Identification of wortmannin-sensitive targets in 3T3-L1 adipocytes. Dissociation of insulin-stimulated glucose uptake and glut4 translocation. J. Biol. Chem. *274*, 24677–24684.

Hill, M.M., Clark, S.F., Tucker, D.F., Birnbaum, M.J., James, D.E., and Macaulay, S.L. (1999). A role for protein kinase Bbeta/Akt2 in insulin-stimulated GLUT4 translocation in adipocytes. Mol. Cell. Biol. *19*, 7771–7781.

James, D.E., Kraegen, E.W., and Chisholm, D.J. (1985). Effects of exercise training on in vivo insulin action in individual tissues of the rat. J. Clin. Invest. *76*, 657–666.

Jiang, Z.Y., Zhou, Q.L., Coleman, K.A., Chouinard, M., Boese, Q., and Czech, M.P. (2003). Insulin signaling through Akt/protein kinase B analyzed by small interfering RNA-mediated gene silencing. Proc. Natl. Acad. Sci. USA *100*, 7569–7574.

Katome, T., Obata, T., Matsushima, R., Masuyama, N., Cantley, L.C., Gotoh, Y., Kishi, K., Shiota, H., and Ebina, Y. (2003). Use of RNA interference-mediated gene silencing and adenoviral overexpression to elucidate the roles of AKT/protein kinase B isoforms in insulin actions. J. Biol. Chem. *278*, 28312–28323.

Khayat, Z.A., Tong, P., Yaworsky, K., Bloch, R.J., and Klip, A. (2000). Insulin-induced actin filament remodeling colocalizes actin with phosphatidylinositol 3-kinase and GLUT4 in L6 myotubes. J. Cell Sci. *113*, 279–290.

Kohn, A.D., Summers, S.A., Birnbaum, M.J., and Roth, R.A. (1996). Expression of a constitutively active Akt Ser/Thr kinase in 3T3-L1 adipocytes stimulates glucose uptake and glucose transporter 4 translocation. J. Biol. Chem. *271*, 31372–31378.

Kohn, A.D., Barthel, A., Kovacina, K.S., Boge, A., Wallach, B., Summers, S.A., Birnbaum, M.J., Scott, P.H., Lawrence, J.C., Jr., and Roth, R.A. (1998). Construction and characterization of a conditionally active version of the serine/threonine kinase Akt. J. Biol. Chem. *273*, 11937–11943.

Kotani, K., Ogawa, W., Matsumoto, M., Kitamura, T., Sakaue, H., Hino, Y., Miyake, K., Sano, W., Akimoto, K., Ohno, S., and Kasuga, M. (1998). Requirement of atypical protein kinase clambda for insulin stimulation of glucose uptake but not for Akt activation in 3T3-L1 adipocytes. Mol. Cell. Biol. *18*, 6971–6982.

Lampson, M.A., Racz, A., Cushman, S.W., and McGraw, T.E. (2000). Demonstration of insulin-responsive trafficking of GLUT4 and vpTR in fibroblasts. J. Cell Sci. *113*, 4065–4076.

Larance, M., Ramm, G., Stockli, J., van Dam, E.M., Winata, S., Wasinger, V., Simpson, F., Graham, M., Junutula, J.R., Guilhaus, M., and James, D.E. (2005). Characterization of the role of the Rab GTPase-activating protein AS160 in insulin-regulated GLUT4 trafficking. J. Biol. Chem. *280*, 37803–37813.

Li, B., Desai, S.A., MacCorkle-Chosnek, R.A., Fan, L., and Spencer, D.M. (2002). A novel conditional Akt 'survival switch' reversibly protects cells from apoptosis. Gene Ther. *9*, 233–244.

Li, M., and Rossi, J.J. (2005). Lentiviral vector delivery of siRNA and shRNA encoding genes into cultured and primary hematopoietic cells. Methods Mol. Biol. *309*, 261–272.

Mitra, P., Zheng, X., and Czech, M.P. (2004). RNAi-based analysis of CAP, Cbl, and CrkII function in the regulation of GLUT4 by insulin. J. Biol. Chem. *279*, 37431–37435.

Molero, J.C., Jensen, T.E., Withers, P.C., Couzens, M., Herzog, H., Thien, C.B., Langdon, W.Y., Walder, K., Murphy, M.A., Bowtell, D.D., et al. (2004). c-Cbl-deficient mice have reduced adiposity, higher energy expenditure, and improved peripheral insulin action. J. Clin. Invest. *114*, 1326–1333.

Sano, H., Kane, S., Sano, E., Miinea, C.P., Asara, J.M., Lane, W.S., Garner, C.W., and Lienhard, G.E. (2003). Insulin-stimulated phosphorylation of a Rab GTPase-activating protein regulates GLUT4 translocation. J. Biol. Chem. *278*, 14599–14602.

Scheid, M.P., Marignani, P.A., and Woodgett, J.R. (2002). Multiple phosphoinositide 3-kinase-dependent steps in activation of protein kinase B. Mol. Cell. Biol. *22*, 6247–6260.

Shewan, A.M., van Dam, E.M., Martin, S., Luen, T.B., Hong, W., Bryant, N.J., and James, D.E. (2003). GLUT4 recycles via a trans-Golgi network (TGN) subdomain enriched in Syntaxins 6 and 16 but not TGN38: involvement of an acidic targeting motif. Mol. Biol. Cell *14*, 973–986.

Tanti, J.F., Grillo, S., Gremeaux, T., Coffer, P.J., Van Obberghen, E., and Le Marchand-Brustel, Y. (1997). Potential role of protein kinase B in glucose transporter 4 translocation in adipocytes. Endocrinology *138*, 2005–2010.

van Dam, E.M., Govers, R., and James, D.E. (2005). Akt activation is required at a late stage of insulin-induced GLUT4 translocation to the plasma membrane. Mol. Endocrinol. *19*, 1067–1077.

Whiteman, E.L., Cho, H., and Birnbaum, M.J. (2002). Role of Akt/protein kinase B in metabolism. Trends Endocrinol. Metab. *13*, 444–451.